

Electronic Supplementary Information

Emissive Covalent Organic Frameworks with Abundant Interaction Sites for Hydrazine Sensing

Yuwei Zhang,^a Ce Xing,^a Zhibin Tian,^b Wanyi Zhao,^a Yongfeng Zhi,^{*b} Lina Zhao,^{*a} and He Li^{*c}

^a Laboratory of Preparation and Applications of Environmental Friendly Materials (Jilin Normal University), Ministry of Education, Changchun, 130103, China, E-mail: zhaolina1975@163.com.

^b School of Chemistry and Chemical Engineering, Hainan University, Haikou, 570228, China, E-mail: zhiyf@hainanu.edu.cn.

^c Division of Energy Materials, Dalian Institute of Chemical Physics, Chinese Academy of Sciences, Dalian 116023, China, E-mail: lihe@dicp.ac.cn.

Characterization

Fourier transform infrared (FT IR) spectra were recorded on a JASCO model FT IR-6100 infrared spectrometer. X-ray diffraction (XRD) data were recorded on a Bruker D8 Focus Powder X-ray Diffractometer by using powder on glass substrate, from $2\theta = 1.5^\circ$ up to 30° with 0.02° increment. Solid-state NMR spectra were obtained with a Bruker 500 MHz spectrometer equipped with a magic-angle spin probe using a 4 mm ZrO_2 rotor. EDS Elemental analysis was performed on a Euro Vector EA3000 elemental analyzer. Nitrogen sorption isotherms were measured at 77 K with a TriStar II instrument (Micromeritics). The Brunauer-Emmett-Teller (BET) method was utilized to calculate the specific surface areas. By using the non-local density functional theory (NLDFT) model, the pore volume was derived from the sorption curve. Morphology images were characterized with a Zeiss Merlin Compact field emission scanning electron microscope (FE-SEM) at an electric voltage of 5 KV.

Synthesis of EH-COF-1

A 10 mL Pyrex tube was charged with 1,3,5-tris(3'-methoxy-4'-hydrazinecarbonylphenyl)benzene (TMHB) (28.5 mg, 0.05 mmol) and 1,3,5-triformyl benzene (TFB) (8.1 mg, 0.05 mmol), dioxane (0.5 mL), mesitylene (0.5 mL), and AcOH (0.1 mL, 6 M), the mixture was sonicated for 1 min, degassed through three freeze-pump-thaw cycles. The system was heated at 120°C for 72 h. The COF was isolated by washed with tetrahydrofuran and acetone, soxhleted with tetrahydrofuran for 12 h, and dried under vacuum for 10 h to afford a white powder in 87% isolated yield.

Synthesis of EH-COF-2

A 10 mL Pyrex tube was charged with 1,3,5-tris(3'-methoxy-4'-hydrazinecarbonylphenyl)benzene (TMHB) (28.5 mg, 0.05 mmol) and 2-hydroxybenzene-1,3,5-tricarbaldehyde (TFB-OH) (8.9 mg, 0.05 mmol), dioxane (0.5 mL), mesitylene (0.5 mL), and AcOH (0.1 mL, 6 M), the mixture was sonicated for 1 min, degassed through three freeze-pump-thaw cycles. The system was heated at 120°C for 72 h. The COF was isolated by washed with tetrahydrofuran and acetone, soxhleted with tetrahydrofuran for 12 h, and dried under vacuum for 10 h to afford a yellow powder in 83% isolated yield.

Luminescence Quenching Experiments

EH-COFs samples were readily dispersed in PBS buffer and the obtained suspension was almost transparent. Moreover, the fluorescence spectra of then active EH-COFs in water solutions were recorded immediately. After adding substance, the fluorescence spectra were observed until the luminescence spectra did not show any change. Each test was repeated for three times to get average values.

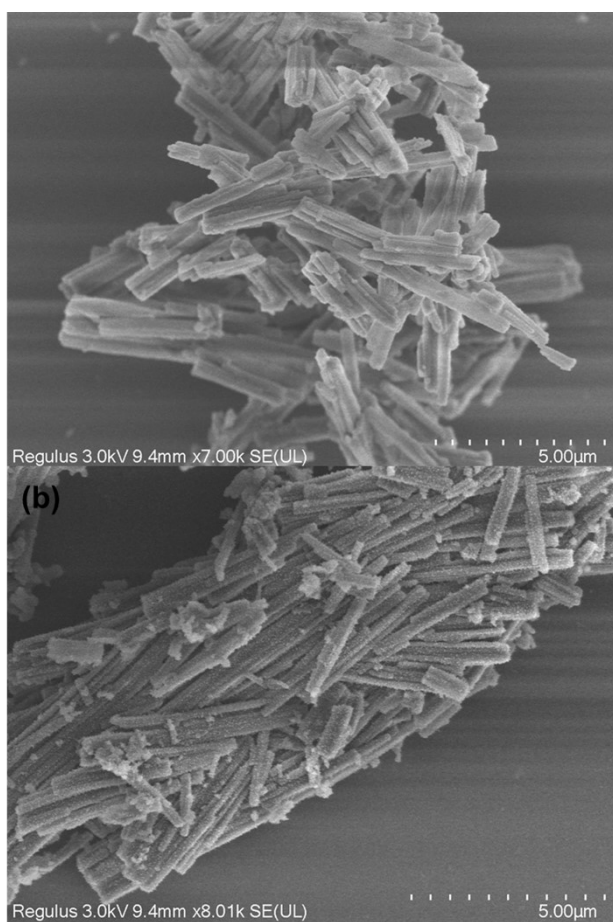


Fig. S1. FE SEM images of (a) EH-COF-1 and (b) EH-COF-2.

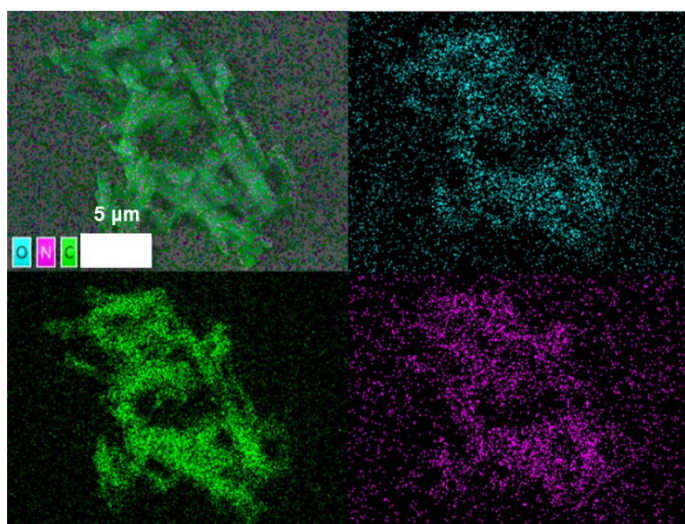


Fig. S2. EDS mapping images of EH-COF-1.

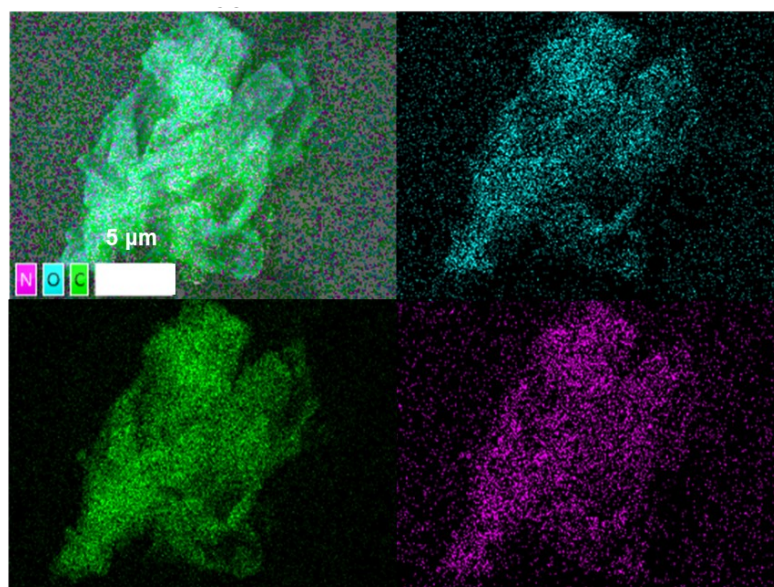


Fig. S3. EDS mapping images of EH-COF-2.

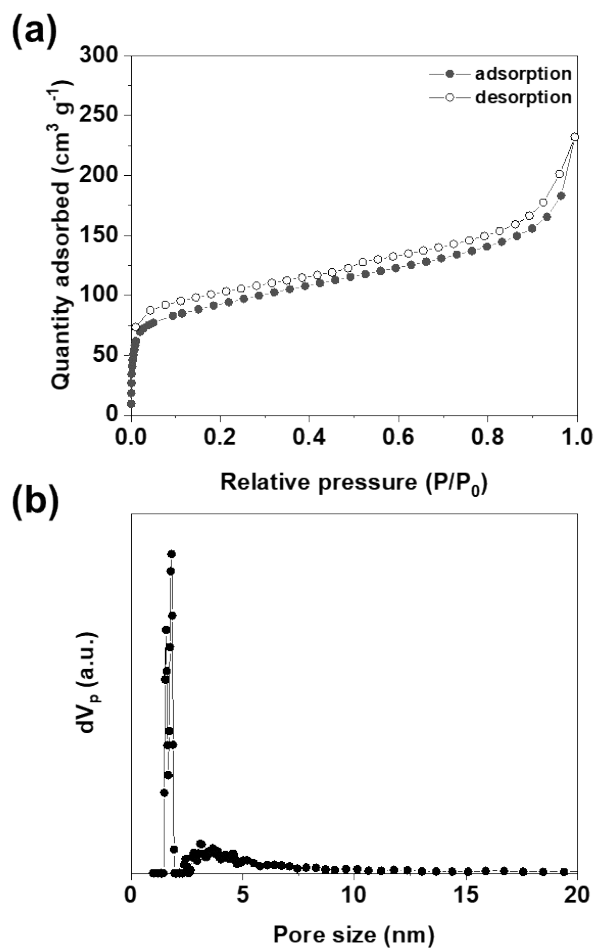


Fig. S4. (a) Nitrogen adsorption–desorption isotherms of EH-COF-1 measured at 77 K. (b) Pore size distribution of EH-COF-1.

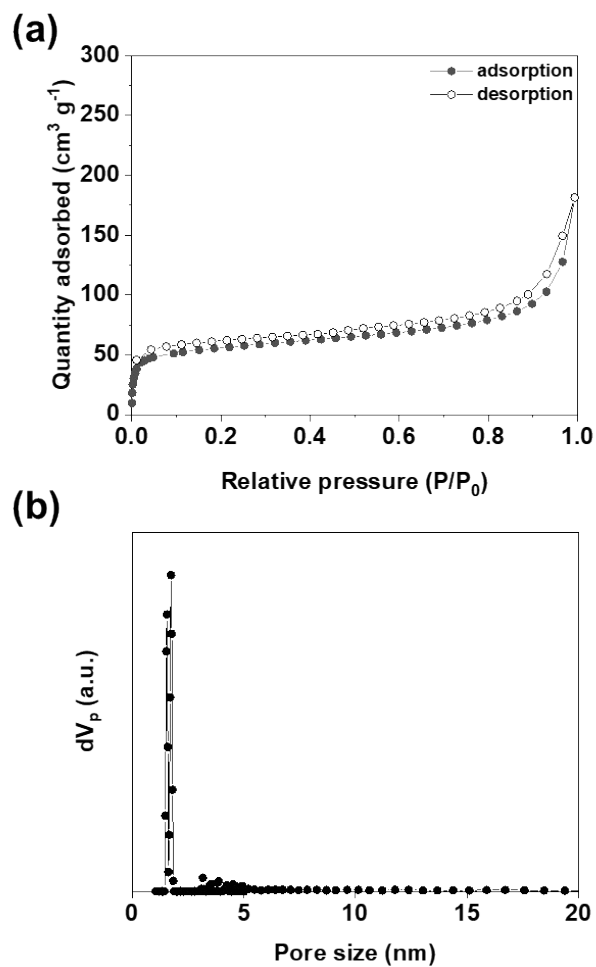


Fig. S5. (a) Nitrogen adsorption–desorption isotherms of EH-COF-2 measured at 77 K. (b) Pore size distribution of EH-COF-2.

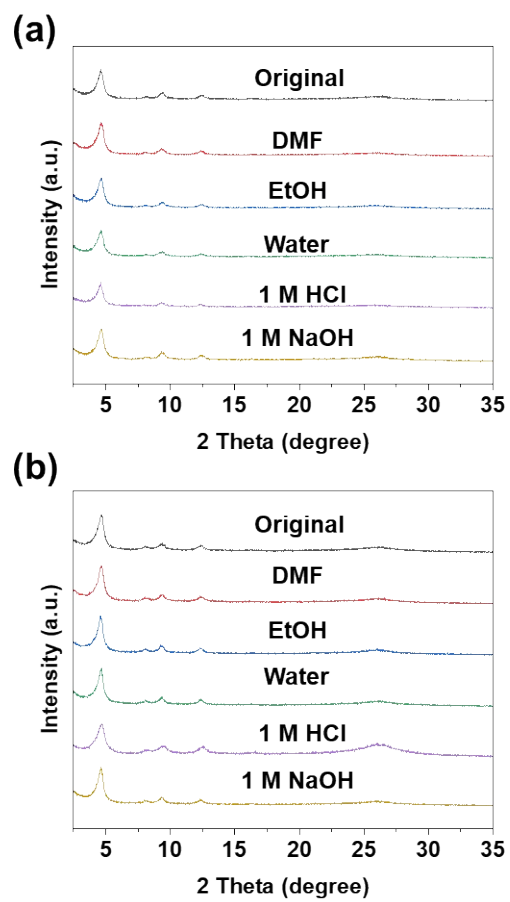


Fig. S6. PXR D patterns of (a) EH-COF-1 and (b) EH-COF-2 under different conditions.

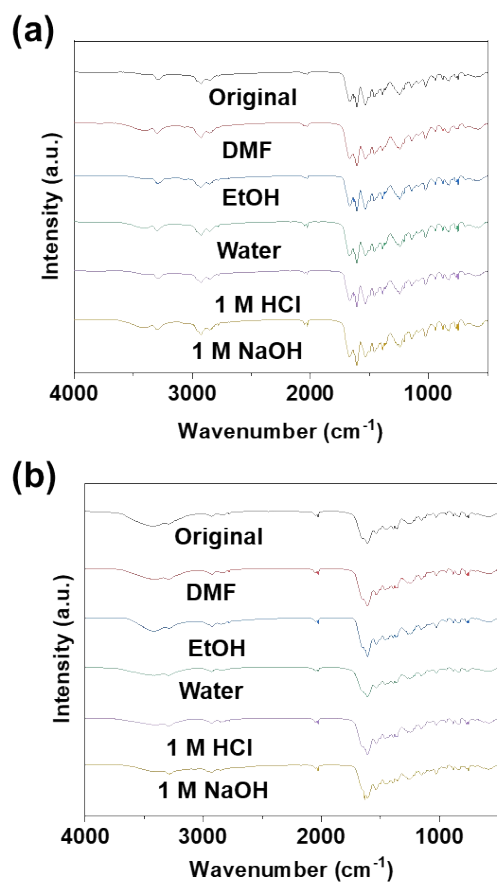


Fig. S7. FT-IR spectra of (a) EH-COF-1 and (b) EH-COF-2 under different conditions.

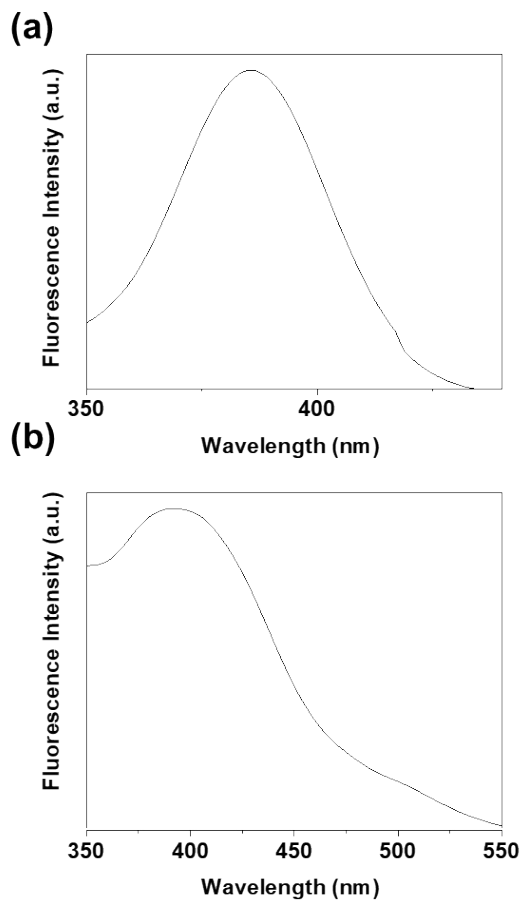


Fig. S8. Excitation spectra of (a) EH-COF-1 and (b) EH-COF-2.

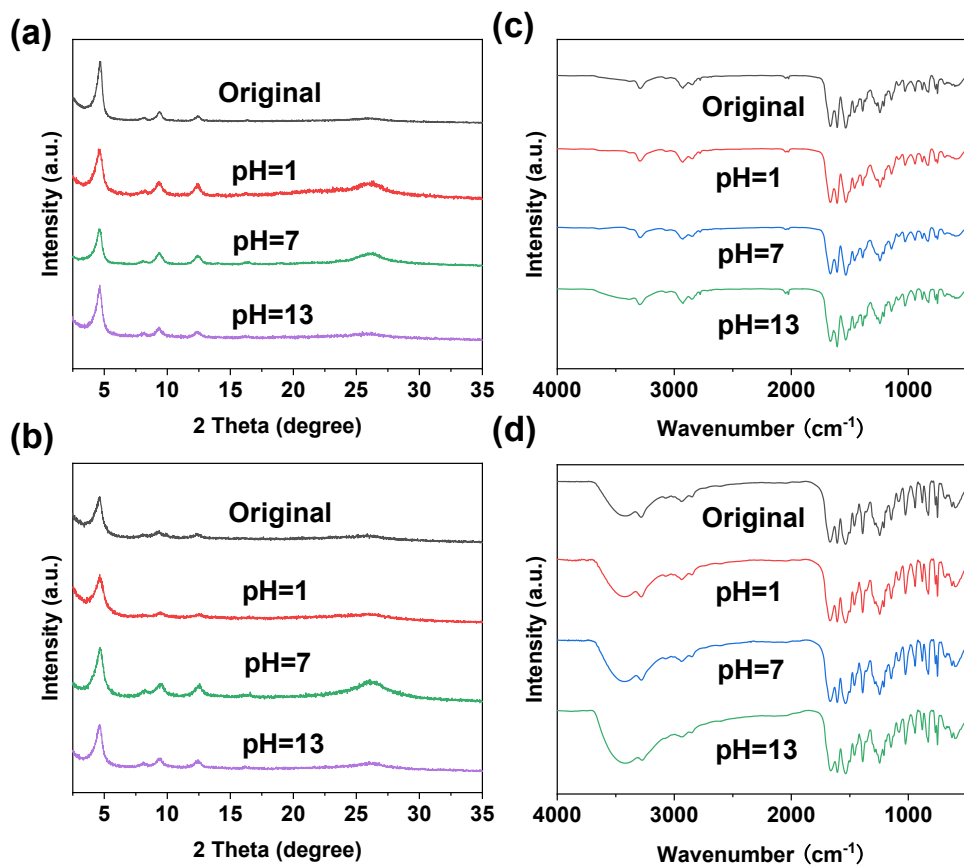


Fig. S9. PXR patterns of (a) EH-COF-1 and (b) EH-COF-2 under different conditions. FT-IR spectra of (c) EH-COF-1 and (d) EH-COF-2 under different conditions.

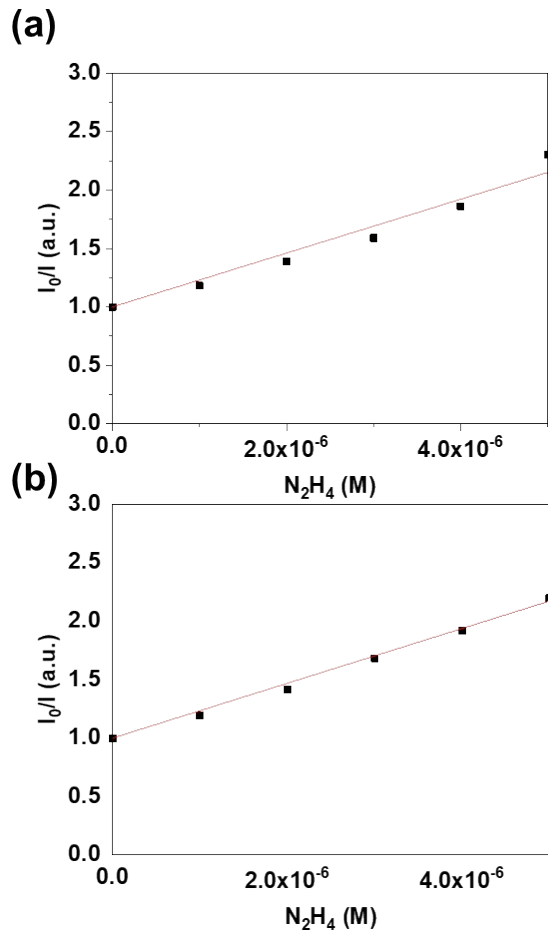


Fig. S10. Plot of PL quenching efficiency (I_0/I) of (a) EH-COF-1 and (b) EH-COF-2 as a function of hydrazine concentration.

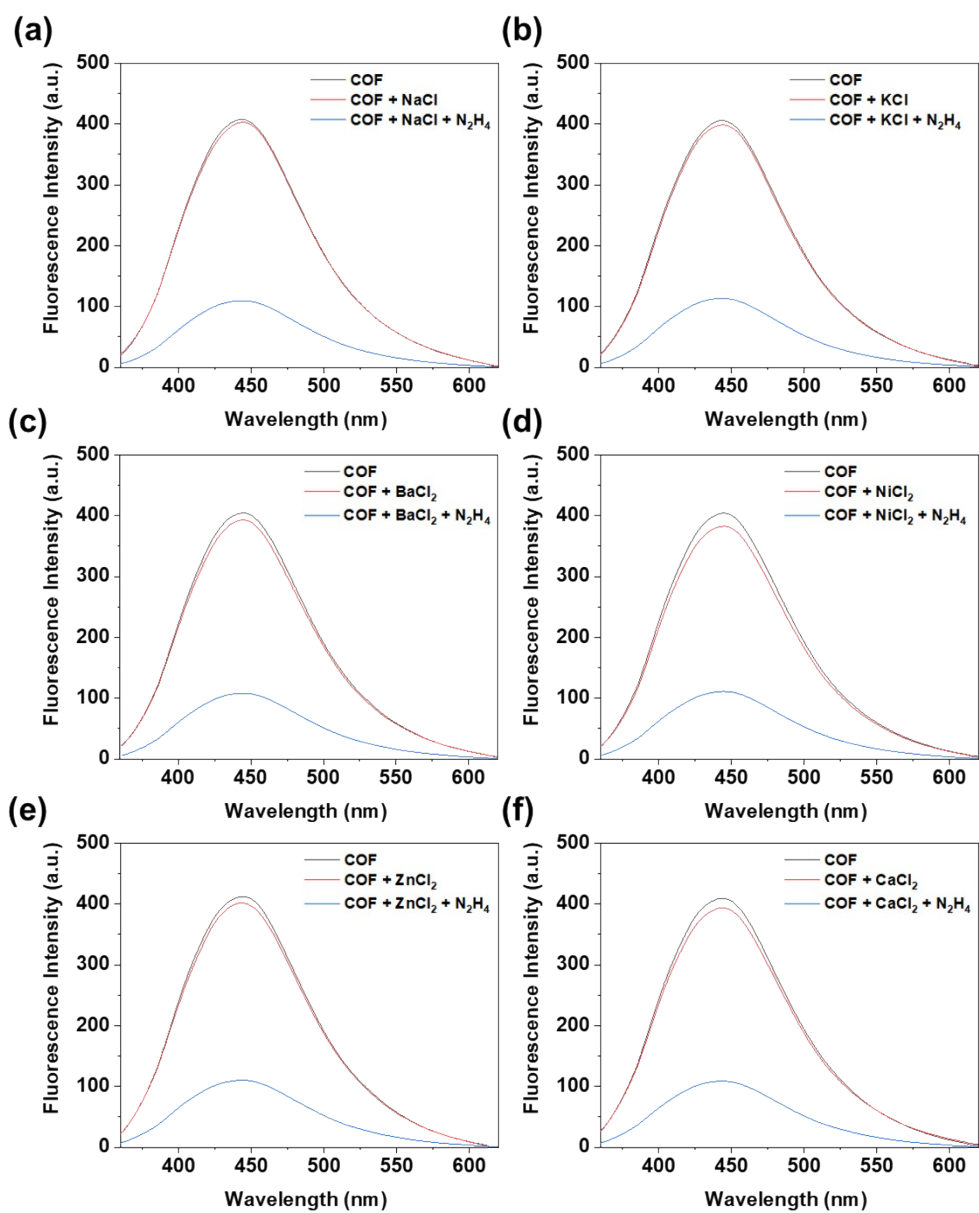


Fig. S11. PL spectra of EH-COF-1 under different ions with/without hydrazine.

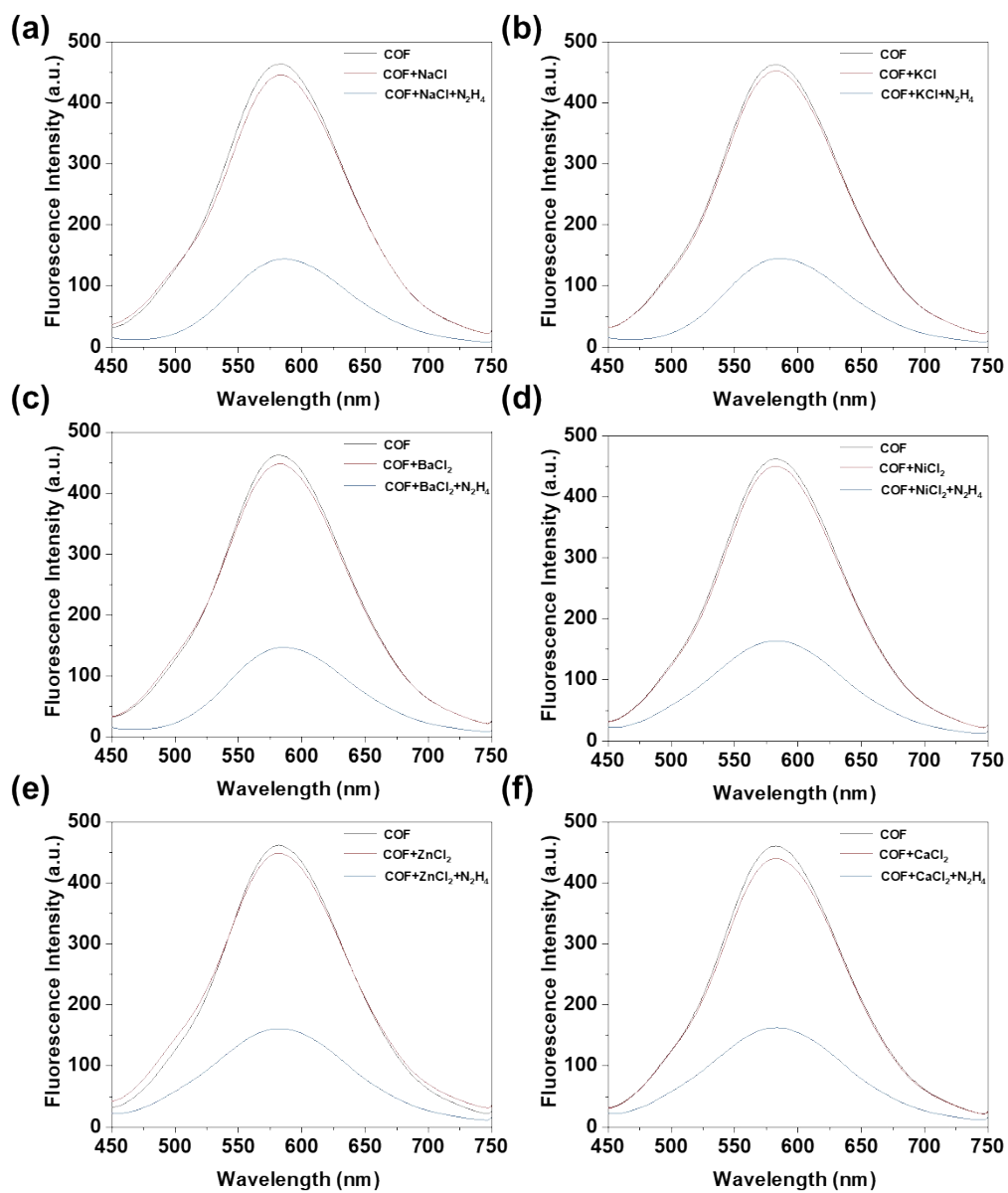
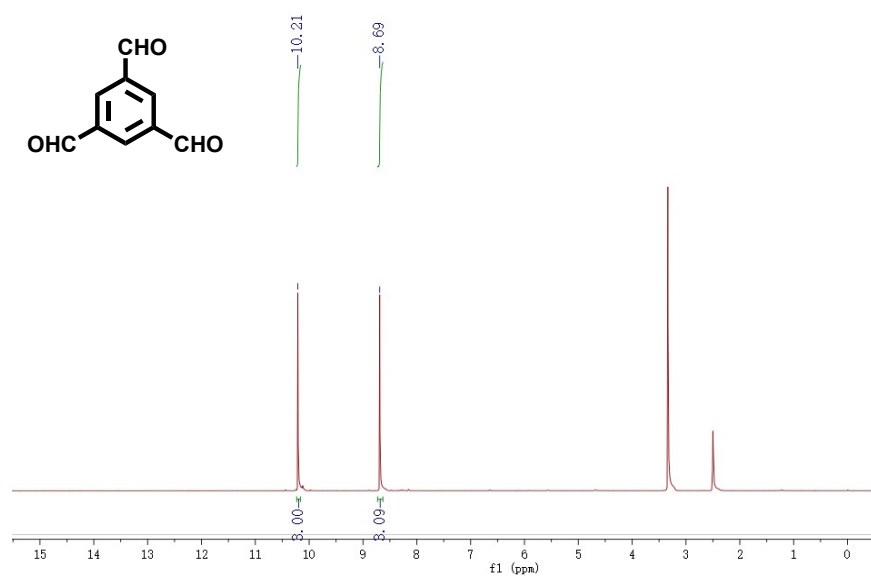
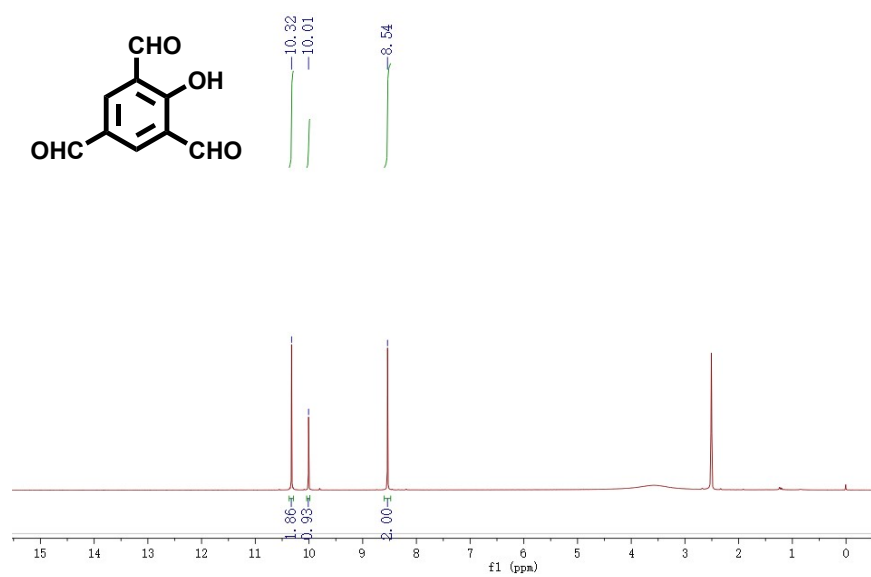


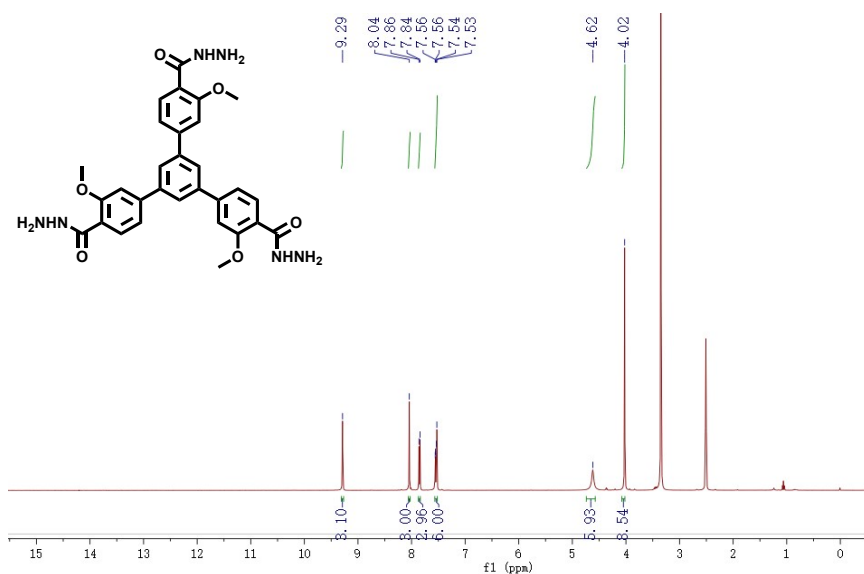
Fig. S12. PL spectra of EH-COF-2 under different ions with/without hydrazine.



Scheme S1. Chemical structure and ¹H NMR spectrum of TFB.



Scheme S2. Chemical structure and ¹H NMR spectrum of TFB-OH.



Scheme S3. Chemical structure and ^1H NMR spectrum of TMHB.

Table S1. Sensing performance of the previous studies.

Sample	LOD (nM)	Ref
COF-TzDha-AC	38000	<i>Sensor Actuat. B-Chem.</i> , 2021, 346, 130472.
TAPB-DHE	400	<i>J. Polym. Sci.</i> , 2023, 62, 1609-1620.
COP-Ta	160000	<i>J. Mater. Chem. C</i> , 2022, 10, 2807-2813.
DAAQ-TFP COF	70	<i>J. Hazard. Mater.</i> , 2020, 381, 120983.
Zr-UiO-66-(OCOCH ₃) ₂	78.8	<i>Dalton Trans.</i> , 2020, 49, 12565-12573.
Zn-MOF	2000	<i>New J. Chem.</i> , 2018, 42, 12486-12491.
Eu ³⁺ @UiO-66-(COOH) ₂	180	<i>RSC Advances.</i> , 2018, 8, 17471-17476.
AuNPs@NPG-rGO	96	<i>Sensor Actuat B-Chem.</i> , 2019, 285, 607-616.
EH-COF-2	28	This work